

Self-assembled structures in block copolymer/graft copolymer blends with hydrogen bonding interaction†

Cite this: *Soft Matter*, 2013, 9, 1756

Yen-Tzu Chen and Chieh-Tsung Lo*

Received 5th November 2012

Accepted 6th December 2012

DOI: 10.1039/c2sm27545g

www.rsc.org/softmatter

The effect of hydrogen bonding on the phase behavior of PS-based block copolymer and poly(styrene-graft-acrylic acid) (PS-*g*-PAA) blends was investigated. The presence of hydrogen bonding enhanced the compatibility of two copolymers. This caused PS-*g*-PAA to intervene in the interface between microdomains of the block copolymer. Consequently, an order–disorder transition occurred at a high concentration of PS-*g*-PAA. On the other hand, poor miscibility and the lack of hydrogen bonding in the blends prevented PS-*g*-PAA from being incorporated into microdomains of the block copolymer, causing the macrophase separation of two copolymers.

Self-assembly spontaneously creates structures or patterns with a significant order parameter. Of these self-assembly materials, block copolymers show microphase separated morphologies on the length scale of nanometer, and are an important class of materials.^{1,2} Investigations have been carried out on the study of linear block copolymers and the phase behavior of these systems is well understood.^{2,3} Although block copolymers provide rich phase behavior and ordered phases, it remains desirable to search for the possibility of producing more varied phases from polymers. Recently, branched copolymers with complex architectures have attracted considerable attention not only due to their importance in understanding the relationship of architectures with properties but also due to their potential applications as interface compatibilizers, thermoplastic elastomers, and viscosity modifiers. Among them, graft copolymers, which consist of a backbone and side chains, have been viewed as novel materials to exhibit unique properties. This is due to their capability to modify the molecular properties of graft copolymers by varying their flexibility, length, and areal density of side chains. In addition, the manipulation of intermolecular interactions between the backbone and side chains by hydrogen or ionic

bonding can offer an even more interesting concept to design graft copolymers with unique properties.^{4,5}

New synthetic approaches allow the preparation of graft copolymers with well-defined molecular architectures.^{6,7} These methods provide precise control over the molecular properties of both the backbone and side chains. However, synthesizing these complex graft copolymers requires high skill, more efforts, and high cost. Currently, polymer blends have been widely applied in many industrial aspects because of their superior properties and ease of modifying the properties of materials. For instance, block copolymer/homopolymer blends show the localization of the homopolymer within the microdomains of the chemically identical block. However, this limits both the size and morphological control of the microdomains. In contrast, binary blends of microphase-separated block copolymers can give rise to a very complex morphology because they may undergo both microphase and macrophase separations, depending on the molecular parameters of the constituent blocks. As we know, the microphase behavior can also be controlled by changing the architecture of polymers. Thus, the replacement of the block copolymer by a branched copolymer can also offer a strategy for the manipulation of the phase behavior of polymer blends. Furthermore, blends consisting of a branched copolymer can provide even more molecular parameters to fine tune the ultimate morphology of blends. Inspired by this idea, we present a study to investigate the microstructures assembled *via* a mixture of graft copolymer and block copolymer. While the graft copolymer exhibits a branched structure that causes the entropic penalty during mixing when compared to block copolymer/homopolymer blends, it is far more difficult to prepare block copolymer/graft copolymer blends without macrophase separation. In this study, we modulated the miscibility between the two copolymers through hydrogen bonding. The concept of using hydrogen bonds to achieve a high level of hierarchy in a microstructure was widely studied in other systems, including block copolymer/homopolymer^{8–12} and block copolymer/block copolymer blends.^{13–16} However, this strategy has never been used by other groups on blends composed of branched copolymers. In this study, we intend to justify the influence of hydrogen bonding on the phase behavior of

Department of Chemical Engineering, National Cheng Kung University, No. 1, University Road, Tainan City 701, Taiwan. E-mail: tsunglo@mail.ncku.edu.tw; Fax: +886-6-2344496; Tel: +886-6-2757575 ext. 62647

† Electronic supplementary information (ESI) available: FTIR of PS-*b*-PEO/PS-*g*-PAA, PS-*b*-PVP/PS-*g*-PAA, and PS-*b*-PMMA/PS-*g*-PAA blends. See DOI: 10.1039/c2sm27545g

Table 1 Characteristics of copolymers used in this study

Polymer	Molecular weight	PDI ^a
Polystyrene- <i>graft</i> -polyacrylic acid (PS- <i>g</i> -PAA)	M_n of PS = 11 500, M_n of PAA = 2300	1.46
Polystyrene- <i>block</i> -polyethylene oxide (PS- <i>b</i> -PEO)	M_n of PS = 40 000, M_n of PEO = 35 000	1.08
Polystyrene- <i>block</i> -poly(2-vinyl pyridine) (PS- <i>b</i> -PVP)	M_n of PS = 40 500, M_n of PVP = 40 000	1.10
Polystyrene- <i>block</i> -poly(methyl methacrylate) (PS- <i>b</i> -PMAA)	M_n of PS = 40 000, M_n of PMMA = 44 000	1.09

^a PDI is the polydispersity index.

block copolymer/*graft* copolymer blends based on a model system of polystyrene-*graft*-polyacrylic acid (PS-*g*-PAA) *graft* copolymer blended with PS based block copolymers of different hydrogen bonding strengths. The achievement in this study will facilitate the design of nanomaterials or biomaterials with complex architecture or tailor the phase behavior of *graft* copolymers to obtain stable and ordered morphologies.

PS based block copolymers and PS-*g*-PAA were provided by Polymer Source, Inc. The properties of the materials are shown in Table 1. A 2% (w/v) polymer solution comprising PS based block copolymers and the PS-*g*-PAA *graft* copolymer with different compositions was mixed in THF ($\geq 99.9\%$, Aldrich Chemical Co., Inc.). The solutions were stored at room temperature for at least three days. The solutions were then cast on both Kapton and epoxy resin to make bulk blends. After 1 day of drying at 50 °C in a vacuum, the blends were annealed at 170 °C for a week.

SAXS measurements were performed at Sector 23A1 at the National Synchrotron Radiation Research Center in Taiwan. Samples on Kapton were measured at room temperature with a sample to detector distance of 2 m. The data were corrected for incident flux, absorption, detector sensitivity variation, and dark current. To complement the SAXS results, TEM images of the blends were obtained. For TEM measurements, specimens embedded in epoxy resin were microtomed to ~ 80 nm thickness. To increase the contrast between the microdomains of copolymers, PS-*b*-P2VP/PS-*g*-PAA blends were selective-stained using iodine for 1 day and both PS-*b*-PEO/PS-*g*-PAA and PS-*b*-PMMA/PS-*g*-PAA blends were treated by OsO₄ for 2 days. The cross-section of the blends was imaged using a Hitachi H7500 electron microscope with an accelerating voltage of 80 kV.

Fig. 1 shows the SAXS data of neat PS-*b*-PEO and its blends with PS-*g*-PAA. For the neat PS-*b*-PEO, the SAXS profile exhibited organized peaks with peak ratios of 1 : 2 : 3, indicating the formation of a lamellar structure. Complementarily, the TEM image for the neat PS-*b*-PEO in Fig. 1(b) matches ideally to the structure obtained by SAXS. Infrared studies (Fig. S1†) show that the (C–O–C) band center of the PEO blocks in the mixture shifts from 1109 cm^{−1} to a lower wavenumber of 1104 cm^{−1}, which is attributed to hydrogen bonding between the ether oxygens of PEO blocks and the carboxylic acid groups of PAA.¹⁷ The formation of hydrogen bonds promotes the compatibility of two blocks. When 10% PS-*g*-PAA was incorporated into PS-*b*-PEO, the blend still formed lamellae as evidenced from SAXS patterns. The lamellar structure remained until 40% PS-*g*-PAA was added into PS-*b*-PEO. In this composition, all

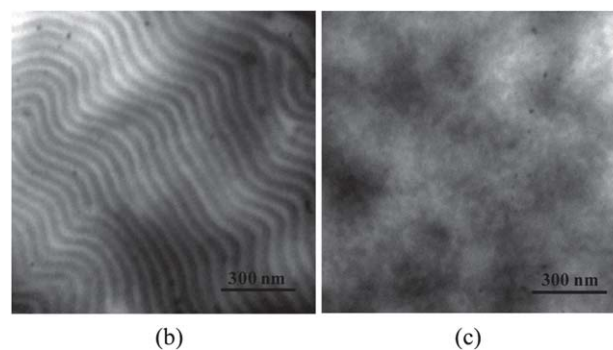
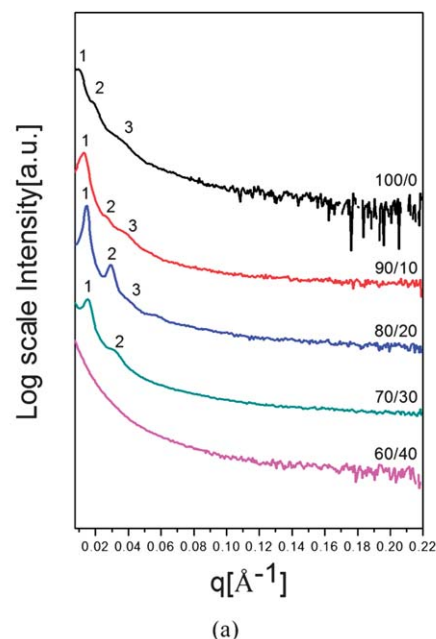


Fig. 1 (a) SAXS of PS-*b*-PEO/PS-*g*-PAA blends; (b) TEM micrographs of neat PS-*b*-PEO; and (c) PS-*b*-PEO/PS-*g*-PAA = 60/40 (wt%/wt%).

diffraction peaks disappeared, implying that an order–disorder transition occurred upon the addition of PS-*g*-PAA. The TEM image in Fig. 1(c) confirmed a disordered structure of PS-*b*-PEO/PS-*g*-PAA. From Fig. 1(a), the domain size of lamellae calculated by Bragg's law decreased from 647.8 Å for neat PS-*b*-PEO, to 479.6 Å, 439.4 Å, and 408.0 Å for 10%, 20%, and 30% PS-*g*-PAA, respectively. This decrease in the domain size with an increase in the PS-*g*-PAA content could be attributed to the location of PS-*g*-PAA in PS-*b*-PEO. When PS-*g*-PAA is mixed with PS-*b*-PEO, two PS domains are found to be miscible. In the case of PAA and PEO, the hydrogen bonds between PAA and PEO improve the compatibility of two blocks. As a result, PS-*g*-PAA prefers to intervene in the interface between PS and PEO microdomains. By using the average interdomain spacing in the lamellar structure of the polymer phase, the change in the average nearest-neighbor distance of chemical junction points along the interface of the lamellae microdomains (a_j/a_{j0}) can be estimated¹⁸

$$\frac{a_j}{a_{j0}} = \left(\frac{\rho_{j0}}{\rho_j} \right)^{1/2} = \left[\left(\frac{D_0}{D} \right) \phi_{\text{block}}^{-1} \right]^{1/2} \quad (1)$$

where a_{j0} and a_j are the average nearest-neighbor distance between the chemical junctions along the interface without and with the

addition of the graft copolymer, ρ_{j0} and ρ_j are the number of block chains per unit interfacial area for the neat block copolymer and its blend with the graft copolymer, D/D_0 is the average interdomain distance of a blend relative to that for the pure block copolymer, and ϕ_{block} is the volume fraction of the block copolymer. Upon the addition of graft copolymer, a_i/a_{j0} increases to 1.23, 1.36, and 1.51 for 10%, 20%, and 30% PS-*g*-PAA, respectively, indicating that the sequestering of PS-*g*-PAA at the interface expands the chemical junction of PS and PEO blocks, causing the lateral expansion of microdomains parallel to the interface. This in turn compresses the two domains normal to the interface. We have to point out that the disappearance of order-order transition is also associated with the location of PS-*g*-PAA in PS-*b*-PEO. In traditional block copolymer/homopolymer blends, the homopolymer swells only the preferred domains of the block copolymer.^{18–21} The distribution of homopolymer in the preferred domain increases the interfacial curvature, leading to an order-order transition of the ordered microstructure. In PS-*b*-PEO/PS-*g*-PAA blends, since PS-*g*-PAA locates at the interface between PS and PEO in PS-*b*-PEO, the addition of PS-*g*-PAA does not cause bending of the interface and an order-order transition is not induced. Instead, when the free volume at the

interface is saturated, additional PS-*g*-PAA could not be incorporated into PS-*b*-PEO, resulting in an order-disorder transition of the blends.

The phase behavior of PS-*b*-PVP upon the addition of PS-*g*-PAA resembles that of the PS-*b*-PEO/PS-*g*-PAA blends. Fig. 2(a) shows the SAXS data of PS-*b*-PVP/PS-*g*-PAA blends. These SAXS profiles essentially reflect that the lamellar structure gradually disappeared with an increase in PS-*g*-PAA, as shown in the corresponding TEM

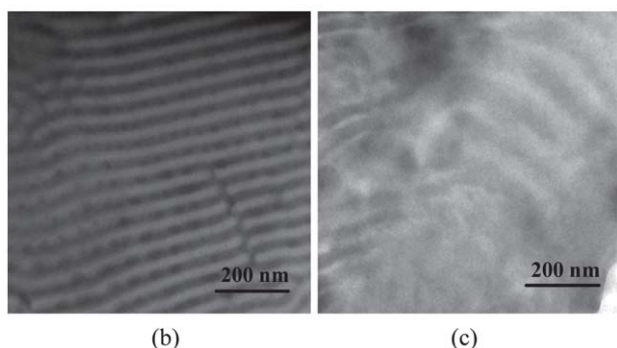
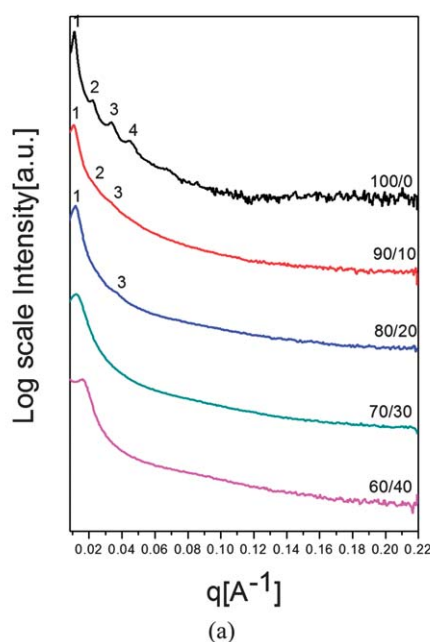


Fig. 2 (a) SAXS of PS-*b*-PVP/PS-*g*-PAA blends; (b) TEM micrographs of PS-*b*-PVP/PS-*g*-PAA = 80/20 (wt%/wt%); and (c) PS-*b*-PVP/PS-*g*-PAA = 70/30 (wt%/wt%).

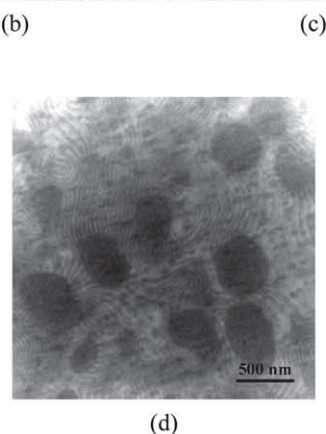
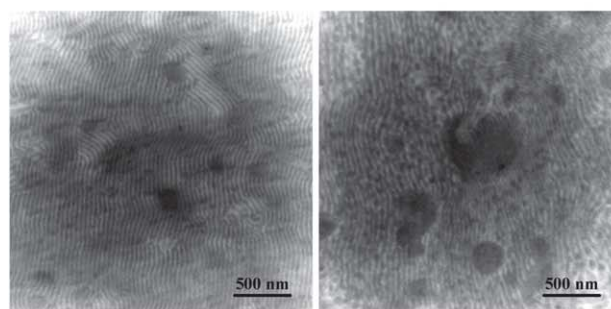
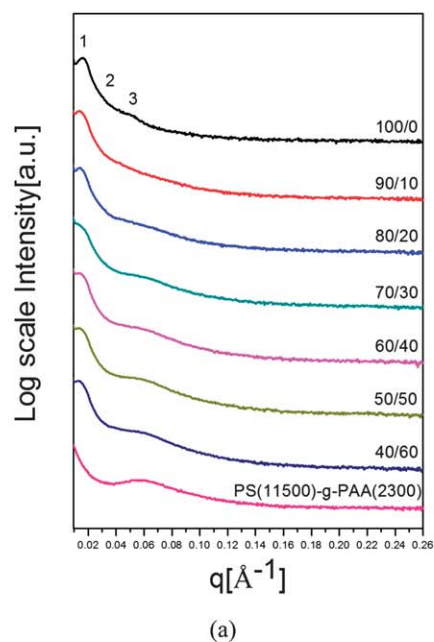


Fig. 3 (a) SAXS of PS-*b*-PMMA/PS-*g*-PAA blends; (b) TEM micrographs of PS-*b*-PMMA/PS-*g*-PAA = 90/10 (wt%/wt%); (c) PS-*b*-PMMA/PS-*g*-PAA = 70/30 (wt%/wt%); and (d) PS-*b*-PMMA/PS-*g*-PAA = 50/50 (wt%/wt%).

images. The TEM image of PS-*b*-PVP/PS-*g*-PAA with a PS-*g*-PAA content of 20% in Fig. 2(b) displays a lamellar structure. When the content of PS-*g*-PAA is increased to 40% (Fig. 2(c)), a disordered morphology was obtained. Similar to the PS-*b*-PEO/PS-*g*-PAA blends, the domain size of PS-*b*-PVP/PS-*g*-PAA blends decreased with an increase in the concentration of PS-*g*-PAA. This behavior implied that the hydrogen bonds between PAA and PVP²² facilitated the positioning of PS-*g*-PAA at the interface between PS and PVP in PS-*b*-PVP. Hence, the interfacial junction of PS and PVP increased and the domain size decreased upon the addition of PS-*g*-PAA.

In PS-*b*-PMMA/PS-*g*-PAA blends, the interaction parameter of PMMA and PAA ($\chi_{\text{PMMA-PAA}}$) at 170 °C calculated by the solubility parameter (δ) (ref. 23) (δ_{PAA} and δ_{PMMA} are 12.0 and 9.45 (cal cm⁻³)^{1/2},²⁴ respectively) is 0.56, suggesting the highly immiscible nature between PMMA and PAA. Additionally, the infrared spectra of carbonyl stretching remain unchanged upon the addition of PMMA, indicating the absence of hydrogen bonds between PAA blocks and PMMA (Fig. S3†). Therefore, the poor compatibility of PS-*b*-PMMA and PS-*g*-PAA is expected. Indeed, SAXS patterns of PS-*b*-PMMA/PS-*g*-PAA blends (Fig. 3(a)) showed different behavior when compared to the other systems. The diffraction peaks originated from the lamellar morphology of PS-*b*-PMMA disappeared at a low PS-*g*-PAA content, and followed by a broad feature occurred at $q \sim 0.06 \text{ \AA}^{-1}$. This broad feature was correlated with the intermolecular interaction of neat PS-*g*-PAA molecules, suggesting that PS-*g*-PAA was phase separated from PS-*b*-PMMA. TEM images in Fig. 3(b)–(d) showed good consistency with the SAXS results. For 10% PS-*g*-PAA in PS-*b*-PMMA, macrophase separation occurred, which was indicated by the dark spots for PS-*g*-PAA and the light region with a lamellar structure for PS-*b*-PMMA. The PS-*g*-PAA region increased upon the addition of PS-*g*-PAA, and the ordered morphology of PS-*b*-PMMA was slowly toward a disordered phase. This macrophase separation of PS-*g*-PAA and PS-*b*-PMMA is the signature of poor compatibility between the two copolymers.

Based on the present finding, the effect of hydrogen bonding on the phase behavior of A-*b*-B block copolymer/A-*g*-C graft copolymer blends is illustrated as shown in Fig. 4. The present blend system consists of two different interactions, including a repulsive interaction between different copolymer chains and an attractive one, originated from hydrogen bonding, in different molecules. In the absence of hydrogen bonds between two immiscible chains, the incompatibility of polymer chains disfavors the enthalpy of mixing and consequently, the graft copolymer is unable to incorporate into the microphase separated domains of the block copolymer. This induces macrophase separation. In contrast, the enhanced miscibility due to the hydrogen bonds between B and C chains reduces the enthalpy of mixing. This facilitates the localization of the graft copolymer at the interface of the block copolymer, forming an ordered structure.

In summary, we demonstrated the possibility of tuning the morphology of block copolymer/graft copolymer blends through hydrogen bonding. Due to the steric effect, the graft copolymer loses the miscibility when it is mixed with the block copolymer. Additionally, the incompatibility between different blocks in copolymers prevents the development of ordered morphology. Through hydrogen bonding, we can position the graft copolymer at the interface of the block copolymer, which prolongs the ordered

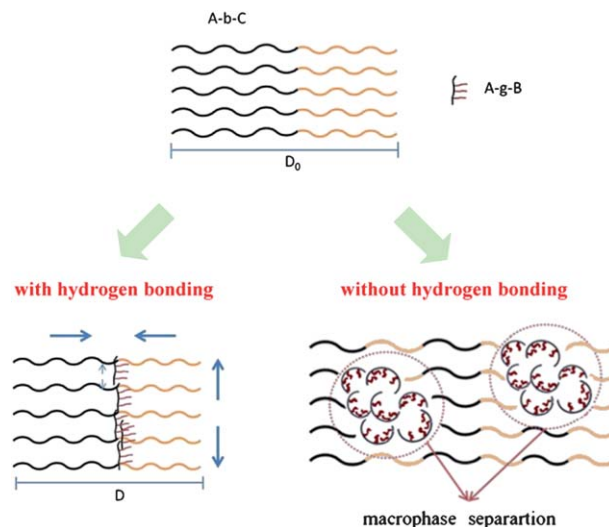


Fig. 4 Schematic illustration of organization of the graft copolymer in the block copolymer.

morphology of the block copolymer upon the addition of graft copolymer. In contrast, without the hydrogen bonding, the low compatibility between two copolymers drives them to macrophase separation. This destructs the ordered structure of the block copolymer.

Acknowledgements

This work was funded by National Science Council in Republic of China under Grant no. NSC 99-2628-E-006-001 and NSC 100-2628-E-006-001.

Notes and references

- 1 F. S. Bates and G. H. Fredrickson, *Phys. Today*, 1999, **52**, 32.
- 2 I. W. Hamley, in *The Physics of Block Copolymers*, Oxford Science Publications, Oxford, UK, 1998.
- 3 V. Abetz, in *Encyclopedia of Polymer Science and Technology*, ed. J. I. Kroschwitz, John Wiley & Sons, 2003, vol. 1.
- 4 O. Ikkala and G. ten Brinke, *Science*, 2002, **295**, 2407.
- 5 J. Ruokolainen, R. Mäkinen, M. Torkkeli, T. Mäkelä, R. Serimaa, G. ten Brinke and O. Ikkala, *Science*, 1998, **280**, 557.
- 6 S. P. Gido, C. Lee, D. J. Pochan, S. Pispas, J. W. Mays and N. Hadjichristidis, *Macromolecules*, 1996, **29**, 7022.
- 7 C. Lee, S. P. Gido, Y. Poulos, N. Hadjichristidis, N. B. Tan, S. F. Trevino and J. W. Mays, *J. Chem. Phys.*, 1997, **107**, 6460.
- 8 J. Q. Zhao, E. M. Pearce and T. K. Kwei, *Macromolecules*, 1997, **30**, 7119.
- 9 Y.-K. Han, E. M. Pearce and T. K. Kwei, *Macromolecules*, 2000, **33**, 1321.
- 10 K. Dobrosielska, S. Wakao, A. Takano and Y. Matsushita, *Macromolecules*, 2008, **41**, 7695.
- 11 W.-C. Chen, S.-W. Kuo, U.-S. Jeng and F.-C. Chang, *Macromolecules*, 2008, **41**, 1401.
- 12 S.-C. Chen, S.-W. Kuo, U.-S. Jeng, C.-J. Su and F.-C. Chang, *Macromolecules*, 2010, **43**, 1083.

- 13 S. Jiang, A. Copfert and V. Abetz, *Macromolecules*, 2003, **36**, 6171.
- 14 T. Asari, S. Matsuo, A. Takano and Y. Matsushita, *Macromolecules*, 2005, **38**, 8811.
- 15 T. Asari, S. Arai, A. Takano and Y. Matsushita, *Macromolecules*, 2006, **39**, 2232.
- 16 Y. Matsushita, *Macromolecules*, 2007, **40**, 771.
- 17 W. P. Gao, Y. Bai, E.-Q. Chen, Z.-C. Li, B.-Y. Han, W.-T. Yang and W.-F. Zhou, *Macromolecules*, 2006, **39**, 4894.
- 18 T. Hashimoto, H. Tanaka and H. Hasegawa, *Macromolecules*, 1990, **23**, 4378.
- 19 H. Tanaka, H. Hasegawa and T. Hashimoto, *Macromolecules*, 1991, **24**, 240.
- 20 K. I. Winey, E. L. Thomas and L. J. Fetters, *J. Chem. Phys.*, 1991, **95**, 9367.
- 21 K. I. Winey, E. L. Thomas and L. J. Fetters, *Macromolecules*, 1992, **25**, 2645.
- 22 J. Dai, S. H. Gou, S. Y. Lee and K. S. Siow, *Polym. J.*, 1994, **26**, 905.
- 23 G. M. Bristow and W. F. Watson, *Trans. Faraday Soc.*, 1958, **54**, 1731.
- 24 L. H. Sperling, in *Introduction to Physical Polymer Science*, Wiley-Interscience, New York, 3rd edn, 2001.